

Revisiting Big-Bang Nucleosynthesis Constraints on Dark-Matter Annihilation

Masahiro Kawasaki^(a,b), Kazunori Kohri^(c,d), Takeo Moroi^(b,e),
and Yoshitaro Takaesu^(e)

^(a) *Institute for Cosmic Ray Research, The University of Tokyo, Kashiwa 277-8582, Japan*

^(b) *Kavli IPMU (WPI), UTIAS, The University of Tokyo, Kashiwa 277-8583, Japan*

^(c) *Theory Center, IPNS, KEK, Tsukuba 305-0801, Japan*

^(d) *Sokendai, Tsukuba 305-0801, Japan*

^(e) *Department of Physics, University of Tokyo, Tokyo 113-0033, Japan*

Abstract

We study the effects of dark-matter annihilation during the epoch of big-bang nucleosynthesis on the primordial abundances of light elements. We improve the calculation of the light-element abundances by taking into account the effects of anti-nucleons emitted by the annihilation of dark matter and the interconversion reactions of neutron and proton at inelastic scatterings of energetic nucleons. Comparing the theoretical prediction of the primordial light-element abundances with the latest observational constraints, we derive upper bounds on the dark-matter pair-annihilation cross section. Implication to some of particle-physics models are also discussed.

Recent cosmological and astrophysical observations have revealed that about 26% of the mass density of the present universe is occupied by dark matter [1]. This fact suggests that there exists a stable (or very long-lived) particle or field which behaves as a non-relativistic object in the present universe. However, the particle-physics nature of dark matter is almost unknown yet, and it is an important task to acquire information about it.

From particle-physics point of view, a stable particle has attracted many attentions as a candidate for dark matter; in our analysis, we assume that some stable particle plays the role of dark matter and denote it as X . In order for an efficient production of the dark-matter particle in the early universe, it is often the case that X has interactions with some of the standard-model particles. In such a case, we may derive constraints on the properties of dark matter by studying the effects of dark-matter pair annihilation into standard-model particles in the early universe.

One of the important effects of dark-matter pair-annihilation is on the big-bang nucleosynthesis (BBN). If dark matter pair-annihilates into charged particles during or after the BBN, they induce photodissociation processes of light elements synthesized via the BBN reactions. In addition, energetic hadrons are often produced as a consequence of the pair-annihilation; if so, hadrodissociation of the light elements are induced. Because the standard BBN scenario predicts the light-element abundances which are more-or-less consistent with observations, too large pair annihilation cross section is excluded. Indeed, such a constraint has been intensively discussed in literatures [2, 3, 4, 5, 6, 7, 8].^{#1}

Recently, there have been progresses in the observational determination of the primordial abundances of the light elements. In particular, uncertainty in the primordial deuterium (D) abundance has been significantly reduced. Such a progress has a large impact on the BBN bounds on the dark-matter properties.

In this letter, we revisit the BBN constraint on the annihilation cross section of dark matter, taking into account the recent progresses in the observation of the light-element abundances. For a reliable calculation of the light-element abundances, we improve the treatment of hadrodissociation; in particular, we have newly included the effects of anti-nucleons emitted by the annihilation of dark matter as well as the effects of interconversion between neutron and proton at inelastic scatterings of energetic nucleons. Then, comparing the theoretical predictions with observational constraints on the light-element abundances, we derive upper bounds on the annihilation cross section of dark matter.

We first summarize the current status of the observational constraints on the primordial abundances of light elements. The primordial abundance of D is inferred from D absorption in damped Ly α systems (DLAs). Recently Cook *et al.* [10] observed a DLA toward QSO SDSS J1358+6522 and performed very precise measurement of D. They also reanalyzed other four previously known DLAs and, using the total five DLA samples, obtained the primordial D abundance as

$$(D/H)_p = (2.53 \pm 0.04) \times 10^{-5}, \quad (1)$$

^{#1}Besides photodissociation and hadrodissociation, annihilation of light dark matter ($m_X \lesssim O(10)$ MeV) affects the BBN by changing the temperature ratio between neutrinos and photons, from which constraints are obtained [9].

where (A/B) denotes the ratio of number densities of light elements A and B, and p indicates the primordial value. Notice that the error is smaller by a factor of 5 than that adopted in our previous study [6]. This progress in the measurement of D leads to more stringent constraints on dark-matter annihilation as seen later.

As for the primordial mass fraction, Y_p , of helium 4 (${}^4\text{He}$), a new determination with the use of the infrared as well as visible ${}^4\text{He}$ emission lines in 45 extragalactic HII regions was reported in Ref. [11], where $Y_p = 0.2551 \pm 0.0022$ is obtained. More recently, Aver, Olive and Skillman [12] reanalyzed the data of Ref. [11] and estimated the ${}^4\text{He}$ abundance using Markov chain Monte-Carlo analysis. They obtained

$$Y_p = 0.2449 \pm 0.0040, \quad (2)$$

which we adopt in this letter.

We also use a constraint on ${}^3\text{He}/\text{D}$ which is derived from D and ${}^3\text{He}$ abundances observed in protosolar clouds [13]; taking into account that the ratio ${}^3\text{He}/\text{D}$ increases monotonically in time, we adopt

$$({}^3\text{He}/\text{D})_p < 0.83 + 0.27. \quad (3)$$

This observational constraint is the same adopted in Ref. [6].

In the previous studies, constraint based on the lithium 7 (${}^7\text{Li}$) abundance was also discussed. However, the situation of the ${}^7\text{Li}$ observation is now confusing. The observed ${}^7\text{Li}$ abundances in metal-poor halo stars showed almost a constant value ($\log_{10}({}^7\text{Li}/\text{H}) \simeq -9.8$) called Spite plateau which was considered as primordial. However, the recent observation found much smaller ${}^7\text{Li}$ abundances ($\log_{10}({}^7\text{Li}/\text{H}) < -10$) for more metal-poor stars [14]. Since we do not know any mechanism to explain such small abundances, we do not use ${}^7\text{Li}$ to constrain the properties of dark matter in this letter. We do not use ${}^6\text{Li}$ either because ${}^6\text{Li}$ abundance is observed as the ratio to the number density of ${}^7\text{Li}$.

In order to derive constraints on the dark-matter properties, we calculate the primordial abundances of the light elements, taking into account the effects of dark-matter annihilation. Our calculation of the light-element abundances is based on Refs. [15, 16] with the modifications explained below. The Boltzmann equations for the evolution of the light-element abundances have the following form:

$$\frac{dn_A}{dt} + 3Hn_A = \left[\frac{dn_A}{dt} \right]_{\text{SBBN}} + \left[\frac{dn_A}{dt} \right]_{\text{photodis}} + \left[\frac{dn_A}{dt} \right]_{\text{hadrodis}} + \left[\frac{dn_A}{dt} \right]_{p \leftrightarrow n}, \quad (4)$$

where n_A denotes the number density of the light element A , and H is the expansion rate of the universe. Here, $[dn_A/dt]_{\text{SBBN}}$ denotes the effects of the standard BBN reactions while the other terms in the right-hand side are the effects of dark-matter annihilation, i.e., those of photodissociation, hadrodissociation, and $p \leftrightarrow n$ conversion. The reaction rates due to the dark-matter annihilation are proportional to the annihilation rate of dark matter which is given by^{#2}

$$\Gamma_{\text{annihilation}} = n_X \langle \sigma v \rangle, \quad (5)$$

^{#2} In a series of papers [15, 16], the effects of decaying particles had been studied. The Boltzmann equations

where n_X is the number density of dark matter. In addition, $\langle\sigma v\rangle$ is the annihilation cross section, with which the Boltzmann equation for the evolution of the number density of dark matter is given by

$$\frac{dn_X}{dt} + 3Hn_X = \langle\sigma v\rangle (n_{X,\text{eq}}^2 - n_X^2), \quad (6)$$

where $n_{X,\text{eq}}$ is the equilibrium value of the number density of dark matter. We assume that the dark-matter annihilation occurs through an s -wave process so that $\langle\sigma v\rangle$ is independent of the relative velocity of dark-matter particles in the non-relativistic limit. The effects of the pair annihilation do not change n_X significantly during and after the BBN epoch because those epochs are long after the freeze-out time of dark matter. Then we use the following time-evolution of n_X :

$$n_X(t) = \frac{3M_{\text{Pl}}^2 H_0^2 \Omega_X}{m_X} \left(\frac{a(t)}{a_0}\right)^3, \quad (7)$$

where $M_{\text{Pl}} \simeq 2.4 \times 10^{18}$ GeV is the reduced Planck scale, H_0 is the Hubble constant, Ω_X and m_X are the density parameter and the mass of dark matter, respectively, and $a(t)$ and a_0 are the scale factor at the cosmic time t and at present, respectively. (In our numerical calculation, we use $H_0 = 68$ km/sec/Mpc and $\Omega_X h^2 = 0.12$.) $[dn_A/dt]_{\text{photodis}}$, $[dn_A/dt]_{\text{hadrodis}}$, and $[dn_A/dt]_{p \leftrightarrow n}$ are proportional to $n_X^2 \langle\sigma v\rangle$, and the effects of the dark-matter annihilation become more efficient as the annihilation cross section $\langle\sigma v\rangle$ increases. In order not to affect the light-element abundances too much, $\langle\sigma v\rangle$ is bounded from above.

Next, we summarize the new points in the calculation of the light element abundances compared to Refs. [15, 16]: revision of the SBBN reaction rates and the treatment of the hadrodissociations. In the present study, we renewed reaction rates by adopting the results of Ref. [17].^{#3} In order to take into account the uncertainties in the reaction rates, we use the Monte-Carlo simulation to estimate the errors of the light element abundances by assuming that the errors of the reaction rates obey Gaussian distributions.

As for the hadrodissociations, we have improved the treatment of the hadronic showers initiated by injections of energetic hadrons into the thermal plasma, including the following effects:^{#4}

1. Effects of anti-nucleons emitted from dark-matter annihilation.

used in the present analysis can be obtained from those in Ref. [15, 16] by replacing $\Gamma_{\text{decay}} \rightarrow \Gamma_{\text{annihilation}}$, where Γ_{decay} is the decay rate defined in Refs. [15, 16], with properly rescaling the numbers of final-state particles produced by the pair annihilation of dark matter using the fact that two dark matters participate in the pair-annihilation process (instead of one for the decay process).

^{#3} For another recent study of nuclear reaction rates, see also Ref. [18], which we do not use in our analysis because there is a technical difficulty in implementing the errors given in Ref. [18] into our Monte-Carlo analysis.

^{#4}For more details, see Ref. [19].

2. Effects of interconversion reactions between (anti-) neutron and (anti-) proton, with which injected and secondary-produced beam nucleons, as well as target nucleons, change their charges at the time of the inelastic scattering.

Concerning the effects of anti-nucleons, we have considered scatterings of anti-nucleons off the background protons and ${}^4\text{He}$'s. The scatterings of anti-nucleons off the background protons produce high-energy nucleons, which can destroy ${}^4\text{He}$'s and produce copious high-energy daughter particles (i.e., nucleons and light elements). Although the inelastic scatterings of anti-nucleons off ${}^4\text{He}$'s produce high-energy daughter particles as well, we have neglected all the final-state particles of the scatterings in the subsequent calculation because of the lack of sufficient experimental data for those inelastic scatterings. It is expected that the inclusion of such final-state particles would only make the BBN constraints severer, and hence our treatment gives conservative bounds.

With the inclusion of the effects of anti-nucleons, the constraints become stronger by 10% – 30% for $m_X \sim 10 \text{ GeV} - 1 \text{ TeV}$. On the other hand, by the latter effects (i.e., the effects of the interconversions at inelastic scatterings), the constraints become weaker by 50% – 80%. This is due to the fact that a high-energy proton, which is interconverted from a beam neutron, tends to be stopped more easily through electromagnetic interactions in the plasma than the neutron with the same energy.

Now, we are at the position to discuss the bounds on the annihilation cross section of dark matter $\langle\sigma v\rangle$. The effects of the dark-matter annihilation on the BBN depend on the final-state particles produced by the annihilation process. Here, we derive the upper bound on $\langle\sigma v\rangle$, assuming that the annihilation process is dominated by one of the following modes:

- $XX \rightarrow W^+W^-$,
- $XX \rightarrow \bar{q}q$ (with $q = u, d, s, c, b$).

We consider only the cases where the pair annihilation results in the production of two particles with an identical mass. Thus, the energy of individual final-state particles is equal to m_X . For the calculation of the photodissociation rate, it is necessary to acquire the total amount of the energy injection in the form of electromagnetic particles due to the pair annihilation. In addition, the study of the hadrodissociation and the $p \leftrightarrow n$ conversion processes requires energy distributions of hadrons (in particular, proton, neutron, and pions) produced by the annihilation of dark matter. The decay, cascade, and hadronization processes of the standard-model particles are studied by using PYTHIA 8.2 package [20].

Comparing the theoretical predictions of light-element abundances with observational constraints, we derive the bounds on the annihilation cross section $\langle\sigma v\rangle$. The results are shown in Figs. 1 and 2 for W^+W^- and $\bar{q}q$ emissions, respectively.^{#5} On the figures, only the constraints from D and ${}^4\text{He}$ are shown because that from ${}^3\text{He}/\text{D}$ is too weak to show up in the figures. We can see that the constraints from D are much more stringent than those from ${}^4\text{He}$.

^{#5}We have also performed an analysis for the case where the dark matter dominantly annihilates into ZZ . We have found that the bound is almost the same as the case with the W^+W^- final state.

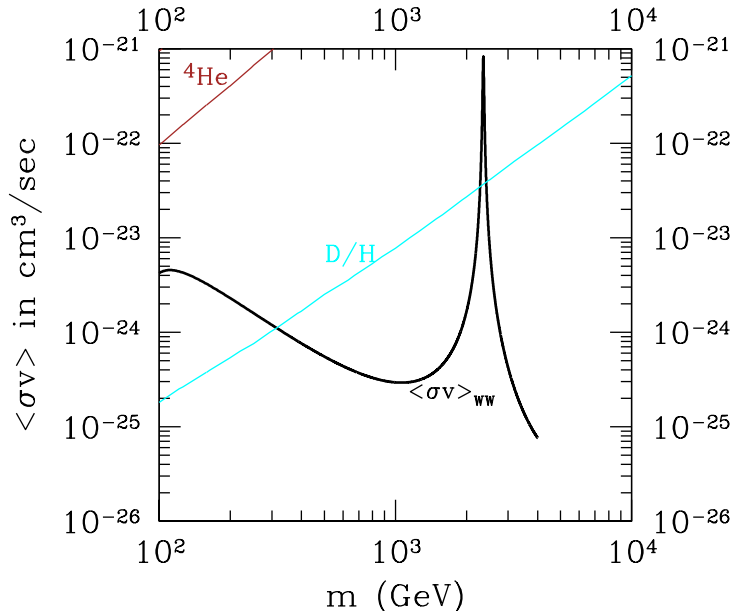


Figure 1: Upper bound at 95% C.L. on the annihilation cross section into the W^+W^- mode as a function of the dark-matter mass. The upper bound comes from the observational deuterium abundance. We also plot the theoretical prediction of the annihilation cross section for a pair of Winos into the W^+W^- mode taken from Ref. [5].

The upper bounds on $\langle\sigma v\rangle$ can be converted to constraints on model parameters once the particle-physics model of dark matter is specified. First, let us consider the case where the neutral Wino \tilde{W}^0 is dark matter in a supersymmetric model. The neutral Wino is the superpartner of the neutral $SU(2)_L$ gauge boson and one of the well-motivated candidates of dark matter, which dominantly pair-annihilates into a W^+W^- pair. In order for the thermal relic Wino to be dark matter, the Wino mass is required to be ~ 3 TeV [21]. However, Wino with smaller mass can also account for dark matter if it is non-thermally produced [22, 23]. In such a case, a larger value of $\langle\sigma v\rangle$ is possible. In Fig. 1, we also plot the cross section for the process $\tilde{W}^0\tilde{W}^0 \rightarrow W^+W^-$ as a function of the dark-matter mass (i.e., the Wino mass). We can see that there exist mass ranges in which the cross section is larger than the upper bound obtained from the BBN. Assuming that neutral Wino is dark matter, the Wino mass is constrained to be

$$320 \text{ GeV} \lesssim M_{\tilde{W}} \lesssim 2.3 \text{ TeV} \quad \text{or} \quad M_{\tilde{W}} \gtrsim 2.5 \text{ TeV}. \quad (8)$$

With the present analysis, the BBN bound on the Wino mass has become more stringent than that obtained in the previous BBN analysis. Neglecting the constraints from ${}^6\text{Li}$ and ${}^7\text{Li}$, the bound was given by $250 \text{ GeV} \lesssim M_{\tilde{W}} \lesssim 2.3 \text{ TeV}$ or $M_{\tilde{W}} \gtrsim 2.4 \text{ TeV}$ [5]. We can

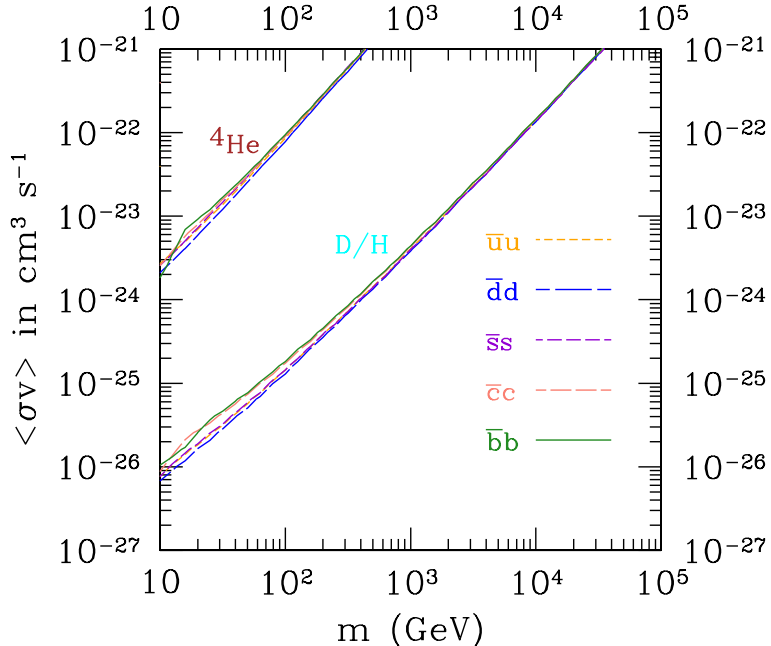


Figure 2: Upper bounds at 95% C.L. on the annihilation cross section into the $\bar{q}q$ mode ($\bar{u}u$, $\bar{d}d$, $\bar{s}s$, $\bar{c}c$, and $\bar{b}b$) as a function of the dark-matter mass. The upper bounds come from the observational deuterium abundance.

see that, in the Wino dark-matter scenario, the lowest possible value of $M_{\tilde{W}}$ is significantly increased. In addition, the scenario of the thermal Wino dark matter (with $M_{\tilde{W}} \simeq 3$ TeV) is allowed. Next, let us discuss the case of thermal relic dark matter, assuming that the dark matter dominantly annihilates into quark pairs. In such a case, $\langle\sigma v\rangle \sim 3 \times 10^{-26} \text{ cm}^3/\text{sec}$ is required, which results in $m_X \gtrsim 25 - 35$ GeV. There are some remarks related with the recent reports of the possible γ -ray line excess from the Galactic center at around GeV energies. In Ref. [24], for example, it is claimed that the signal can be fitted by the $\bar{q}q$ emission from annihilation of dark matter with the mass of 36 – 51 GeV.^{#6} Such a region is still consistent with the BBN bounds.

Finally, let us comment on other collider and astrophysical constraints. One constraint is from the direct search of charged Wino at the LHC experiment. Because the charged and neutral Winos are almost mass-degenerate, the charged Wino becomes relatively long-lived (i.e., $\tau_{\tilde{W}^\pm} \sim O(0.1 \text{ ns})$) if the neutral Wino is the LSP [26, 27]. Then, the charged Wino production may leave disappearing track at the LHC. The bound from the disappearing-track search is currently $M_{\tilde{W}} \gtrsim 270$ GeV at 95% C.L. [28, 29], which is weaker than the BBN bound.

Another constraint is estimated from the study of the energetic γ -ray fluxes from Milky Way satellites. In some case, sizable γ -ray fluxes are expected from those satellites, although no signal has been observed yet. The negative search for the γ -ray signal results in a lower bound on the mass of dark matter. For example, Ref. [30] obtained the constraint of

^{#6}For other efforts, see also Refs. [25].

$320 \text{ GeV} \leq M_{\tilde{W}} \leq 2.25 \text{ TeV}$ or $M_{\tilde{W}} \geq 2.43 \text{ TeV}$ for the Wino dark-matter scenario with the study of four nearby dwarf spheroidal galaxies (dSphs) whose dark-matter profiles can be obtained with stellar kinematic data. In addition, with extra assumptions to determine the dark-matter profiles, the Fermi-LAT collaboration [31] obtained $1 \text{ TeV} \lesssim M_{\tilde{W}} \lesssim 1.7 \text{ TeV}$ or $M_{\tilde{W}} \gtrsim 2.8 \text{ TeV}$. The Fermi-LAT collaboration also obtained $m_X \gtrsim 110$ and 150 GeV for the thermal relic dark matter scenario with W^+W^- and $\bar{q}q$ emissions, respectively. Although these constraints are comparable to or severer than the BBN ones, constraints from γ -ray in general may suffer from uncertainties of the density profiles of dark matter in galaxies.

The recent observation of the anti-proton flux in high-energy cosmic ray [32] also puts a bound on the mass of dark matter [33]. Importantly, however, the theoretical prediction of the anti-proton flux from the dark-matter annihilation has large uncertainty because the anti-proton flux is sensitive to the model of cosmic-ray propagation as well as the dark-matter density profile of the Milky Way. Using the result of Ref. [34], for example, the anti-proton constraint on the Wino dark matter scenario is $M_{\tilde{W}} \gtrsim 240 - 250 \text{ GeV}$. In addition, for the case of $\bar{q}q$ emission for the annihilation process, the mass of dark matter is constrained to be $m_X \gtrsim 20 \text{ GeV}$, assuming the annihilation cross section to realize the thermal relic dark matter scenario. These constraints are weaker than the BBN constraints obtained by our analysis. (However, they may become more stringent if one takes propagation models or density profiles other than that adopted in Ref. [34].)

Since dark-matter annihilation affects the ionization history of the universe, the observations of the cosmic microwave background (CMB) constrain the annihilation cross section. The recent Planck obtained $\langle\sigma v\rangle \lesssim 4 \times 10^{-28} \text{ cm}^3\text{s}^{-1}f^{-1}(m_X/\text{GeV})$ [1], where f is the fraction of the injected energy that goes into the background plasma. f is expected to be $\sim O(0.1)$; for example $f \simeq 0.15$ for the annihilation into $\tau^+\tau^-$ and $f \simeq 0.2$ for the annihilation into $\mu^+\mu^-$ or $b\bar{b}$ [1]. If we take $f \sim 0.2$ as a typical value, the Planck result leads to the constraints, $400 \text{ GeV} \lesssim M_{\tilde{W}} \lesssim 2.1 \text{ TeV}$ or $M_{\tilde{W}} \gtrsim 2.6 \text{ TeV}$ for the Wino dark matter, and $m_X \gtrsim 15 \text{ GeV}$ for the thermal relic dark matter with $q\bar{q}$ emission. (For more accurate bounds, precise calculation of f is necessary for each model.) Therefore, the CMB constraints are comparable to the BBN constraints.

In summary, we have studied effects of dark-matter annihilation in the early universe on the abundances of the light elements synthesized during the BBN epoch. If the dark-matter annihilation results in the production of electromagnetic and hadronic particles, they affect the abundances of the light elements through photodissociation, hadrodissociation, and $p \leftrightarrow n$ conversion processes. We have calculated the abundances of D, ^3He , and ^4He , taking into account above processes. In the study of the effects of dark-matter annihilation, we have improved the treatment of the hadrodissociation processes. In particular, (i) we have included the effects of the anti-nucleon emitted by the annihilation process of dark matter, and (ii) we take account of the interconversion reactions between neutron and proton at inelastic scatterings. Then, comparing the theoretical prediction with the latest observational constraints on the primordial abundances of the light elements, we have derived the upper bounds on the pair annihilation cross section of dark matter. We found that the latest results on the measurements of the D abundance, which result in a precise determination of

the primordial abundance of D, have a strong impact. For the case of Wino dark matter, for example, the BBN constraint requires the Wino mass to be $320 \text{ GeV} \lesssim M_{\tilde{W}} \lesssim 2.3 \text{ TeV}$ or $M_{\tilde{W}} \gtrsim 2.5 \text{ TeV}$.

We thank M. Arnould and P. D. Serpico for useful discussions. This work is supported in part by Grant-in-Aid for Scientific research from the Ministry of Education, Science, Sports, and Culture (MEXT), Japan, Nos. 23104008 (T.M. and Y.T.), 25400248 (M.K.), 26105520 (K.K.), 26247042 (K.K.), 26400239 (T.M.) and 15H05889 (M.K. and K.K.). The work of K.K. is also supported by the Center for the Promotion of Integrated Science (CPIS) of Sokendai (1HB5804100) and World Premier International Research Center Initiative (WPI Initiative), MEXT, Japan (M.K. and T.M.).

References

- [1] P. A. R. Ade *et al.* [Planck Collaboration], arXiv:1502.01589 [astro-ph.CO].
- [2] M. H. Reno and D. Seckel, Phys. Rev. D **37**, 3441 (1988).
- [3] J. A. Frieman, E. W. Kolb and M. S. Turner, Phys. Rev. D **41**, 3080 (1990),
- [4] K. Jedamzik, Phys. Rev. D **70**, 083510 (2004) [astro-ph/0405583].
- [5] J. Hisano, M. Kawasaki, K. Kohri and K. Nakayama, Phys. Rev. D **79**, 063514 (2009) [arXiv:0810.1892 [hep-ph]]; Phys. Rev. D **80**, 029907 (2009) [arXiv:0810.1892 [hep-ph]].
- [6] J. Hisano, M. Kawasaki, K. Kohri, T. Moroi and K. Nakayama, Phys. Rev. D **79**, 083522 (2009) [arXiv:0901.3582 [hep-ph]].
- [7] J. Hisano, M. Kawasaki, K. Kohri, T. Moroi, K. Nakayama and T. Sekiguchi, Phys. Rev. D **83**, 123511 (2011). [arXiv:1102.4658 [hep-ph]].
- [8] B. Henning and H. Murayama, arXiv:1205.6479 [hep-ph].
- [9] K. M. Nollett and G. Steigman, Phys. Rev. D **89**, no. 8, 083508 (2014) [arXiv:1312.5725 [astro-ph.CO]]; Phys. Rev. D **91**, no. 8, 083505 (2015) [arXiv:1411.6005 [astro-ph.CO]].
- [10] R. Cooke, M. Pettini, R. A. Jorgenson, M. T. Murphy and C. C. Steidel, arXiv:1308.3240 [astro-ph.CO].
- [11] Y. I. Izotov, T. X. Thuan and N. G. Guseva, Mon. Not. Roy. Astron. Soc. **445**, 778 (2014) [arXiv:1408.6953 [astro-ph.CO]].
- [12] E. Aver, K. A. Olive and E. D. Skillman, JCAP **1507**, no. 07, 011 (2015) [arXiv:1503.08146 [astro-ph.CO]].

- [13] J. Geiss and G. Gloeckler, *Space Science Reviews* **106**, 3 (2003).
- [14] L. Sbordone, P. Bonifacio, E. Caffau, H.-G. Ludwig, N. T. Behara, J. I. G. Hernandez, M. Steffen and R. Cayrel *et al.*, *Astron. Astrophys.* **522**, A26 (2010) [arXiv:1003.4510 [astro-ph.GA]].
- [15] M. Kawasaki, K. Kohri and T. Moroi, *Phys. Lett. B* **625**, 7 (2005) [astro-ph/0402490]; *Phys. Rev. D* **71**, 083502 (2005) [astro-ph/0408426].
- [16] M. Kawasaki, K. Kohri, T. Moroi and A. Yotsuyanagi, *Phys. Rev. D* **78** (2008) 065011 [arXiv:0804.3745 [hep-ph]].
- [17] P. D. Serpico, S. Esposito, F. Iocco, G. Mangano, G. Miele and O. Pisanti, *JCAP* **0412**, 010 (2004) [astro-ph/0408076].
- [18] Y. Xu, K. Takahashi, S. Goriely, M. Arnould, M. Ohta and H. Utsunomiya, *Nucl. Phys. A* **918**, 61 (2013) [arXiv:1310.7099 [nucl-th]].
- [19] M. Kawasaki, K. Kohri, T. Moroi, and Y. Takaesu, work in progress.
- [20] T. Sjöstrand *et al.*, *Comput. Phys. Commun.* **191**, 159 (2015) [arXiv:1410.3012 [hep-ph]].
- [21] J. Hisano, S. Matsumoto, M. Nagai, O. Saito and M. Senami, *Phys. Lett. B* **646** (2007) 34 [hep-ph/0610249].
- [22] G. F. Giudice, M. A. Luty, H. Murayama and R. Rattazzi, *JHEP* **9812** (1998) 027 [hep-ph/9810442].
- [23] T. Moroi and L. Randall, *Nucl. Phys. B* **570** (2000) 455 [hep-ph/9906527].
- [24] T. Daylan, D. P. Finkbeiner, D. Hooper, T. Linden, S. K. N. Portillo, N. L. Rodd and T. R. Slatyer, arXiv:1402.6703 [astro-ph.HE].
- [25] L. Goodenough and D. Hooper, arXiv:0910.2998 [hep-ph]; D. Hooper and L. Goodenough, *Phys. Lett. B* **697**, 412 (2011) [arXiv:1010.2752 [hep-ph]]; D. Hooper and T. Linden, *Phys. Rev. D* **84**, 123005 (2011) [arXiv:1110.0006 [astro-ph.HE]]; K. N. Abazajian and M. Kaplinghat, *Phys. Rev. D* **86**, 083511 (2012) [*Phys. Rev. D* **87**, 129902 (2013)] [arXiv:1207.6047 [astro-ph.HE]]; D. Hooper and T. R. Slatyer, *Phys. Dark Univ.* **2**, 118 (2013) [arXiv:1302.6589 [astro-ph.HE]]; C. Gordon and O. Macias, *Phys. Rev. D* **88**, no. 8, 083521 (2013) [*Phys. Rev. D* **89**, no. 4, 049901 (2014)] [arXiv:1306.5725 [astro-ph.HE]]; W. C. Huang, A. Urbano and W. Xue, arXiv:1307.6862 [hep-ph]; K. N. Abazajian, N. Canac, S. Horiuchi and M. Kaplinghat, *Phys. Rev. D* **90**, no. 2, 023526 (2014) [arXiv:1402.4090 [astro-ph.HE]]; T. Daylan, D. P. Finkbeiner, D. Hooper, T. Linden, S. K. N. Portillo, N. L. Rodd and T. R. Slatyer, arXiv:1402.6703 [astro-ph.HE].

- [26] J. L. Feng, T. Moroi, L. Randall, M. Strassler and S. f. Su, Phys. Rev. Lett. **83** (1999) 1731 [hep-ph/9904250].
- [27] M. Ibe, S. Matsumoto and R. Sato, Phys. Lett. B **721** (2013) 252 [arXiv:1212.5989 [hep-ph]].
- [28] G. Aad *et al.* [ATLAS Collaboration], Phys. Rev. D **88**, no. 11, 112006 (2013) [arXiv:1310.3675 [hep-ex]].
- [29] V. Khachatryan *et al.* [CMS Collaboration], JHEP **1501**, 096 (2015) [arXiv:1411.6006 [hep-ex]].
- [30] B. Bhattacharjee, M. Ibe, K. Ichikawa, S. Matsumoto and K. Nishiyama, JHEP **1407** (2014) 080 [arXiv:1405.4914 [hep-ph]].
- [31] M. Ackermann *et al.* [Fermi-LAT Collaboration], arXiv:1503.02641 [astro-ph.HE].
- [32] AMS-02 collaboration, talks at the “AMS DAYS AT CERN – The Future of Cosmic Ray Physics and Latest Results,” April 15-17, 2015, CERN.
- [33] G. Giesen, M. Boudaud, Y. Genolini, V. Poulin, M. Cirelli, P. Salati and P. D. Serpico, arXiv:1504.04276 [astro-ph.HE]; H. B. Jin, Y. L. Wu and Y. F. Zhou, arXiv:1504.04604 [hep-ph]; C. Evoli, D. Gaggero and D. Grasso, arXiv:1504.05175 [astro-ph.HE]; M. Ibe, S. Matsumoto, S. Shirai and T. T. Yanagida, Phys. Rev. D **91**, no. 11, 111701 (2015) [arXiv:1504.05554 [hep-ph]]; K. Hamaguchi, T. Moroi and K. Nakayama, Phys. Lett. B **747**, 523 (2015) [arXiv:1504.05937 [hep-ph]]; S. J. Lin, X. J. Bi, P. F. Yin and Z. H. Yu, arXiv:1504.07230 [hep-ph].
- [34] C. Evoli, D. Gaggero and D. Grasso, arXiv:1504.05175 [astro-ph.HE].